Transcriptome analysis and identification of genes associated with chicken sperm storage duration

Liubin Yang, Xinting Zheng, Changhuan Mo, Shaomei Li, Zhiwei Liu, Ge Yang, Qianqian Zhao, Shijun Li,[1] and Chunyan Mou[1]

Key Laboratory of Agricultural Animal Genetics, Breeding and Reproduction, Ministry of Education, Huazhong Agricultural University, Wuhan, Hubei Province, 430070 China

ABSTRACT The sperm storage tubules located in the mucosal folds of the uterovaginal junction (**UVJ**) are the primary site of sperm storage in chicken hens after natural mating or artificial insemination (**AI**). The short-term sperm storage (24 h after mating or AI) in hens was highly associated with immunity and pH-related pathway genes. However, the underlying mechanism of longer duration of sperm storage in female birds remains largely unclear. In the present study, transcriptome analysis was applied to uncover the dynamic gene expression changes in chicken UVJ tissues at two time points (day 3 and day 9) after AI. A total of 574 differentially expressed genes (**DEG**) were enriched, including 266 upregulated and 308 downregulated DEG. The validation of 5 DEG using quantitative PCR showed a similar expression tendency with RNA sequencing results. The gene ontology terms of DEG were highly enriched in heparin binding (9 genes including *COMP*, *CTGF*, and *IMPG2*), glycosaminoglycan binding (10 genes including *PCOLCE*, *POSTN*, and *RSPO3*), and response to estradiol and ion transport (*AREG*, *RAMP3*, *SFRP1*, and *SSTR1*). Kyoto encyclopedia of genes and genomes pathway-enrichment analyses of DEG revealed 10 significant pathways ($P < 0.05$) represented by calcium signaling pathway (7 genes including *CACNA1G*, *PDE1C*, *PDGFRB*, and *SLC8A1*) and glycosaminoglycan biosynthesis (*B3GNT7*, *CSGALNACT1*, *GLCE*, and *ST3GAL1*). Protein-protein interaction network of DEG established the connection-regulating epithelial cell or cell-matrix adhesion and migration. The enriched pathways and genes were highly correlated with temporary sperm storage in and possibly sequential sperm release from chicken UVJ overtime after AI. Of these, *HIP1*, *PDE1C*, and calcium-related genes were the most interesting candidates associated with sperm storage duration. This report provided a global gene expression profile of the chicken UVJ regarding the capacity of sperm storage overtime after AI. The outcome of this study will contribute to further understanding of the long-term sperm maintenance in avian females and eventually improving the duration of fertile egg performance by selected chicken breeding.

Key words: artificial insemination, gene expression, sperm storage tubule, transcriptome, uterovaginal junction

INTRODUCTION

The sperm storage duration is an interesting biological feature that is observed in many female birds. In hens, sperm storage tubules (**SST**) that are dispersed in the mucosal folds of the uterovaginal junction (**UVJ**) in oviduct are the primary site for sperm storage (Bobr, et al., 1964). After mating or artificial insemination (**AI**), the sperms travelled from vagina and entered into SST, where they appeared as packed bundles with their heads directed toward the blind tubular end of SST, and were maintained in the SSTs up to weeks (Gilbert, et al., 1968; Bakst, et al., 1994). The sperms contain highly compact DNA with inactivated transcription. The regulation of sperm function was largely relying on their extracellular environment (Sullivan and Saez, 2013). Previous studies showed that female birds had potential impacts to regulate the metabolic activity and motility of the residing sperms (Bakst and Bauchan, 2015) and to protect the sperms against the immune threats from the female oviduct (Das, et al., 2010). A series of proteins (enzymes) and signals associated with sperm storage have been identified including carbonic anhydrase (Holm, et al., 1996),

aquaporins (Zaniboni and Bakst, 2004), alkaline phosphatase (Bakst and Akuffo, 2007), avidin, avidin-related protein-2, progesterone receptor (Foye-Jackson, et al., 2011), and transforming growth factor-β and its receptors (Das, et al., 2010). The fatty acids (Huang, et al., 2016) and lactic acid (Matsuzaki, et al., 2015) were reported to have a function in sperm storage (Holt and Fazeli, 2016; Matsuzaki and Sasanami, 2017). The detection of high calcium concentration in SST cells and tubular fluid, which was within the range to inhibit the sperm motility, supports the functional role of calcium signaling during the sperm maintenance and storage (Holm, et al., 2000). A handful of immune- and pH-regulatory genes were previously enriched in the transcriptomes of chicken UVJ tissues under the 2 conditions (24 h after mating vs. unmated hens) (Atikuzzaman, et al., 2015; Han, et al., 2019b). These results addressed that the sperm maintenance, selection, and release are complex processes (Matsuzaki and Sasanami, 2017). Although the short-term sperm storage is largely an immediate immune response that is conserved between hens and pigs (Atikuzzaman, et al., 2017), the mechanisms regulating the lengthy tolerance of spermatozoa or long-term sperm storage in the UVJ remain mostly unclear.

In this study, we hypothesized that as the number of sperms gradually decreases in SSTs with ovulatory cycle, factors beyond the immune response and pH, that are highly correlated with sperm activity and sperm-related genes, would be changing accordingly. This report aimed to identify the gene network regulating the long-term sperm storage in UVJ tissues of chicken hens and provide further understanding of long-term sperm maintenance and release in reservoir beyond the immediate immune response.

MATERIALS AND METHODS

Ethics Statement

All animal experiments were carried out following the protocols (No. 5 proclaim of the Standing Committee of Hubei People's Congress) approved by the Standing Committee of Hubei People's Congress and the ethics committee of Huazhong Agricultural University, China.

Sample Collection and RNA Isolation for Transcriptome Sequencing

White Leghorn roosters and hens at the age of 30 wk were raised individually in stair-step cages under standard management system and fed with isocaloric and isonitrogenous corn-soybean–based diet twice a day with enough drinking water. All chickens experienced 16 h of light and 8 h of dark a day.

A total of 11 hens were artificially inseminated with mixed semen after performing the quality and quantity check as described in previous reports (Atikuzzaman, et al., 2015). Each female bird was inseminated with 30 μL of mixed semen on the same day (day 0) and raised

for sample collection on day 3 after AI (5 individuals) and on day 9 after AI (6 individuals). All the selected hens were sacrificed to collect the UVJ tissues containing SST under stereomicroscope. The UVJ tissues were carefully dissected and divided into 2 parts at an angle perpendicular to the ovary-uterus axis. One half of the UVJ tissues were fixed immediately in 4% paraformaldehyde (in phosphate buffered saline) for histological study, while the other half was snap-frozen in liquid nitrogen for RNA isolation.

Histological Study

The histological examination of UVJ tissues was performed following the standard procedures. Briefly, a piece of UVJ tissues or folds containing SST was cut off under the stereomicroscope and submerged in running water for approximately 20 h. Then, samples were sequentially dehydrated, embedded in paraffin, and processed for section at 5-μm thickness using a microtome (Leica Instruments GmbH). The sections were stained by hematoxylin and eosin and photographed by using a microscopy and imaging system (Olympus, Japan).

RNA Isolation and cDNA Preparation

Each frozen UVJ sample was homogenized in 1 mL of TRIzol Reagent to perform RNA isolation and purification (Invitrogen, Carlsbad, CA) according to the manufacturer's protocol. A total of 6 RNA samples (3 samples from day 3 after AI and 3 samples from day 9 after AI) were selected for RNA sequencing program by Novogene Biotechnology Company (NOVOGENE, China). In addition, the total RNA (1 μg) of the samples from 2 groups (2 selected time points) were applied for reverse transcription by using TransScript One-Step gDNA Removal and cDNA Synthesis SuperMix kit (TansGen Biotech, Beijing, China) to perform quantitative PCR validation.

Transcriptome Sequencing and Data Analysis

Sequencing library for mRNA sequencing was carried out following the standard procedure and applied for sequencing using PE-150 at Novogene Biotechnology Company. The sequenced raw data were processed for quality control and mapped to chicken reference genome (ftp://ftp.ensembl.org/pub/release-94/fasta/gallus_gallus/dna/). Index of the reference genome was built, and paired-end clean reads were aligned to the reference genome using Hisat2, version 2.0.5 (Johns Hopkins University Center for Computational Biology, Washington, D.C.). Feature Counts, version 1.5.0-p3 (Bioconductor, Seattle, WA), was used to count the reads mapped to each gene. Then, fragments per kilobase million (FPKM) of each gene was calculated based on the length and reads for estimating gene expression level. Differential expression analysis of 2 groups (3

biological replicates per condition) was performed using the DESeq2 R package (version 1.16.1; Bioconductor). The resulting P values were adjusted using the Benjamini and Hochberg's approach for controlling the false discovery rate. Genes with a P value < 0.05 and | log2 (fold change) | > 0.5 were assigned as threshold for differentially expressed by DESeq2.

Gene Ontology, Kyoto Encyclopedia of Genes and Genomes Enrichment, and Protein-Protein Interaction Analyses of Differentially Expressed Genes.

Gene ontology (**GO**) enrichment analysis of differentially expressed genes (**DEG**) was implemented by the clusterProfiler (3.8) R package (Bioconductor), in which gene length bias was corrected. GO terms with corrected P value < 0.05 were considered to be significantly enriched. clusterProfiler (3.8) R package was used to test the statistical enrichment of DEG in Kyoto Encyclopedia of Genes and Genomes (**KEGG**) pathways. Protein-protein interaction network of DEG in UVJ folds was carried out by the STRING website (https://string-db.org/) at medium confidence (minimum required interaction score: 0.04). Then, data were edited in Cytoscape, version 3.6.1, software (Bethesda, National Institute of General Medical Sciences of the National Institutes of Health).

Analysis of DEGs by Quantitative Real-time PCR

The quantitative real-time PCR primers were designed by the NCBI Primer-BLAST website (https://www.ncbi.nlm.nih.gov/tools/primer-blast/). The primer information was listed in Table S1. Several differentially expressed mRNA were used for quantitative PCR analysis to verify the gene expression tendency in day 3 (n = 5) and day 9 post-AI (n = 6) cDNA samples. The quantitative PCR amplification conditions were as follows: 95°C for 5 min; 39 cycles of 95°C for 15s and 57°C for 15s; 72°C for 15s; 72°C for 5 min. The foldchange was calculated by 2-ΔΔCt method, and the significance testing was conducted by t test.

RESULTS

Histological Observation of Reduced Sperms in SST of UVJ Folds Derived from Mated Hens (day 9 vs. day 3 After AI)

Chicken UVJ is regarded as an important sperm storage site after insemination. To investigate the potential difference relevant to the duration of sperm storage, the UVJ folds containing SSTs of white Leghorn hens were collected on day 3 and day 9 after AI to examine the morphology in the UVJ of the hen oviduct. The mucosa of UVJ folds was characterized as lamina propria and pseudostratified ciliated columnar epithelium that branched into lamina propria to form tubular glands with a single layer of columnar epithelium named SST. The sperms were observed with their heads gathering together as a tightly packed bundle in SST cavity, located closely next to the tubular end and paralleled to SST. The sperm bundles in SST were detected in both sections derived from day 3 and day 9 post-AI samples, whereas the number of SST containing sperm bundles was much less when comparing day 9 samples with day 3 samples (Figure 1). What are the mechanisms governing the dynamic changes remains unclear. Transcriptome sequencing strategy was applied to decipher the genes and networks involved in this progression.

Enrichment of DEGs in UVJ Folds Derived From Mated Hens (day 9 vs. day 3 After AI)

To investigate the molecular mechanisms involved in the decreased sperms in chicken UVJ folds, 2 sets of UVJ folds containing SST that were collected at 2 time points after mating (day 3 and day 9 after AI) with 3 replicates were applied for high throughput RNA sequencing. Illumina sequencing of 6 UVJ tissue samples produced a total of 364,311,924 raw reads and generated 353,509,306 clean reads after quality control (97% of the raw reads). More than 82% of the clean reads were uniquely mapped to the chicken reference genome (Gallus_gallus-5.0) to enrich the DEG between these 2 sets of UVJ samples (day 9 vs. day 3 after AI). A total of 574 genes were identified as differentially expressed genes including 266 upregulated and 308 downregulated transcripts (Figure 2A) and presented in Table S2. Of those, several sperm-related transcripts were enriched and represented as *AGO2*, *ASB9*, *CECR2*, and *FGF13*, as shown in Table 1.

GO Terms, KEGG Pathway Enrichment, and Protein-Protein Interaction Analyses of DEG

The 574 DEG were used to perform GO and KEGG analyses. The GO analysis revealed a total of 381 significant (P < 0.05) enriched terms. The top 30 of 381 GO terms were obtained and presented in Table S3 and Figure 2C. Of those, the most prominent enrichment was heparin binding (*COMP*, *CTGF*, *IMPG2*, *PCOLCE*, *POSTN*, *RSPO3*, *SFRP1*, *TGFBR3*, and *THBS4*) and glycosaminoglycan (GAG) binding (*CEMIP*, *COMP*, *CTGF*, *IMPG2*, *PCOLCE*, *POSTN*, *RSPO3*, *SFRP1*, *TGFBR3*, and *THBS4*)-related terms (q < 0.05) that are highly associated with the characteristics (spermatozoa capacitation) of sperm reservoir (chicken UVJ). In addition, 2 enriched GO terms named as response to estradiol (4 genes enriched) and regulation of metal ion transport (11 genes enriched) were potentially involved in the interaction of oviduct epithelium and sperms to regulate spermatozoa capacitation and sperm release from SST (P < 0.05). There were 2 terms represented as IgE binding (2 genes enriched) and antigen binding (3 genes enriched) that were possibly linked with immune response. The enriched proteinaceous extracellular matrix (12 genes enriched) and regulation
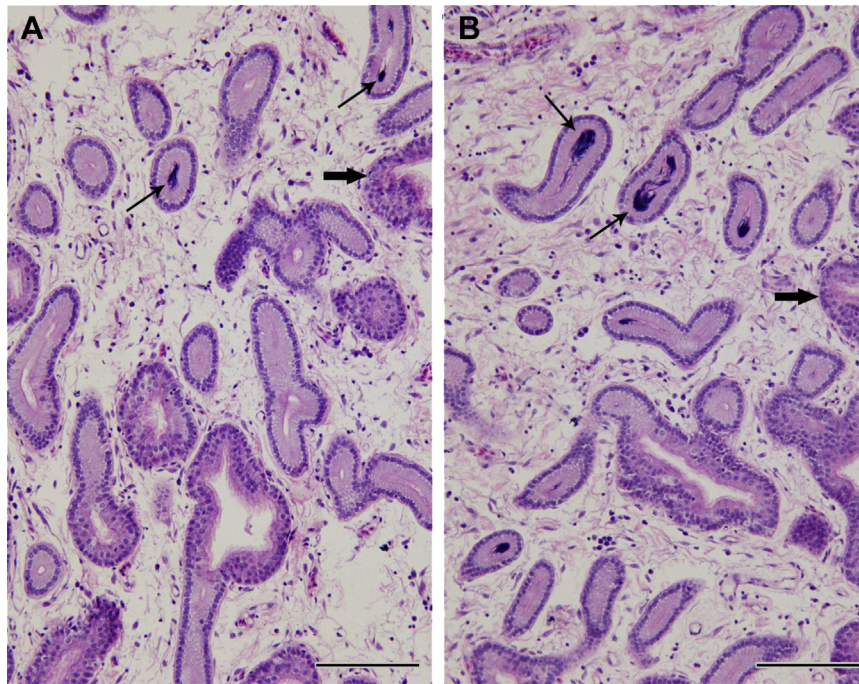
Figure 1. Histological comparison of uterovaginal junction (UVJ) folds containing sperm storage tubules (SST) stained with hematoxylin and eosin between day 3 and day 9 after artificial insemination (AI) in chicken hens. The epithelium of UVJ folds and SST were pseudostratified ciliated columnar (pointed with bold arrows) and simple columnar, respectively. Sperms were gathered and distributed in the lumen of SST (pointed with narrow arrows) as shown in at day 9 (A) and at day 3 (B) post AI. Scale bar = 100 μm.

of peptidase activity (13 genes enriched) and peptidase regulator activity (8 genes enriched) ($P < 0.05$)-related GO terms had a potential impact on the hormone regulation of the microenvironment in SST of UVJ. There were additional 10 calcium-related and 11 ion-related (excluding calcium) GO terms represented as calcium ion binding (18 genes enriched), calcium ion transport (10 genes enriched), calcium ion import (7 genes enriched), regulation of calcium ion transport (8 genes enriched), metal ion transport (18 genes enriched), iron ion binding (7 genes enriched), sodium ion transport (7 genes enriched), and regulation of ion transport (15 genes enriched) that potentially mediate the sperm motility as shown in Table 2.

KEGG pathway enrichment revealed 10 significant pathways ($P < 0.05$) represented by calcium signaling pathway (7 genes enriched) and extracellular matrix (**ECM**)-receptor interaction (6 genes enriched). The top 20 KEGG terms were presented in Figure 2D. Furthermore, 5 signaling pathways that potentially regulate the sperm storage in UVJ including calcium signaling pathway (7 genes enriched), GAG biosynthesis keratan sulfate (4 genes enriched), ECM-receptor interaction (6 genes enriched), and glutathione metabolism (3 genes enriched) were enriched (Table 3). The most promising candidates displayed the decreasing expression tendency, including *PDE1C* gene.

Protein-protein interaction network established a broad interconnection regulating epithelial cell or cell-matrix adhesion and migration centered by *FN1*, *POSTN*, and *SDC1*. The other 2 subnetworks

potentially contributing to ion binding or transport including *NOS1* and *SLC39A11*, and the protein releasing or inflammatory response mediated by G-protein coupled receptors *GRM4*, *SSTR1*, and *P2RY6*, were also set up as shown in Figure 2B.

Quantitative Real-time PCR Validation of Candidate Genes Regulating the Sperm Storage Capacity of Chicken UVJ

To gain the information of dynamic gene expression changes occurring in the chicken UVJ folds containing SST after AI, we performed quantitative PCR to evaluate the reliability of our RNA-seq result, and a total of 5 genes (*CACNA1G*, *CFTR*, *HIP1*, *PIGZ*, and *ST3GAL1*) were randomly selected for detailed investigation of gene expression patterns by using the quantitative PCR technique. The downregulation of *CACNA1G* and *ST3GAL1* and the upregulation of *CFTR*, *PIGZ*, and *HIP1* in UVJ of mated chicken hens (day 9 vs. day3) were consistent with the tendency of RNA sequencing results (Figure 3).

DISCUSSION

Sperm reservoir is widely accepted as the temporary location for sperm maintenance in female reproductive tracts in many animals, such as cows, pigs, reptiles, insects, and birds (Matsuzaki and Sasanami, 2017). In mated chicken hens, a large amount of spermatozoa
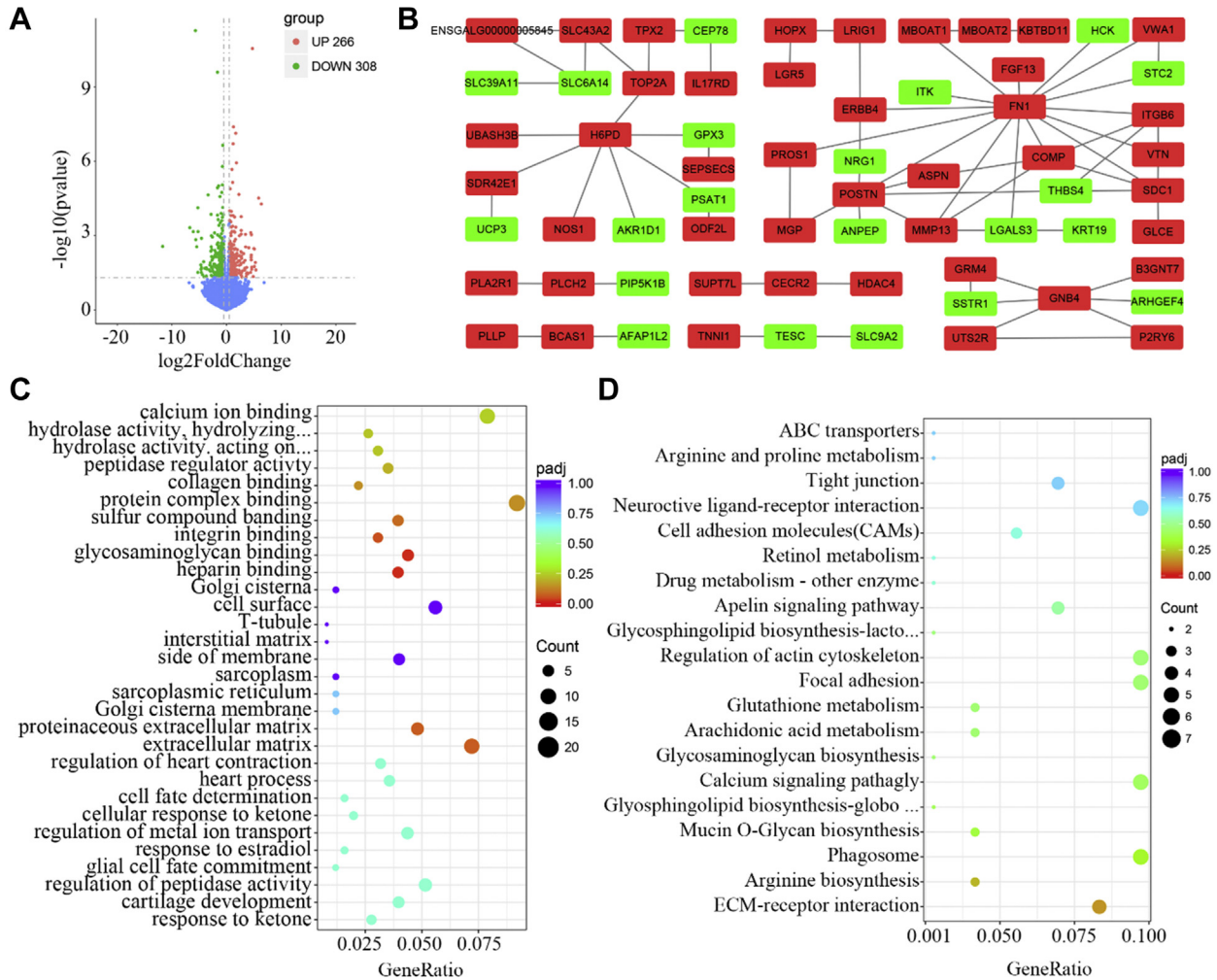
Figure 2. (A) The volcano plots of differentially expressed genes (DEG) enriched in chicken uterovaginal junction (UVJ) folds containing sperm storage tubules (SST) (day 9 vs. day 3 after artificial insemination [AI]). The X-axis and Y-axis represented the log2 fold change values and the statistical significance P values ($-\log10$), respectively. The red and green dots represented upregulated and downregulated mRNA expression of DEG, with expression exceeding the threshold value within log2 fold change values between 0.5 and -0.5, P value < 0.05. The blue dots represented the genes with expression level beyond the stated threshold of P value < 0.05. (B) Protein-protein interaction network of DEG in mated chicken UVJ folds (day 9 vs. day 3 after AI). Network nodes and edges represented proteins and protein-protein associations, respectively. The red and green nodes represented downregulated and upregulated genes, respectively. (C) The top 30 enriched biological processes of DEG comparing the UVJ containing SST at day 9 to day 3 after AI. (D) The top 20 enriched Kyoto Encyclopedia of Genes and Genomes (KEGG) pathways of DEG in UVJ comparing between day 9 and day 3 after AI.

were supposed to experience sequential processes including escaping the immune attack at the site of vagina, travelling to the UVJ for short-term or long-term stay, engineering progressive release from the UVJ to the uterus, and migrating upward to infundibulum to meet the oocyte and reach the final destination for successful fertilization (Gilbert, et al., 1968; Bakst, et al., 1994). The detailed movements of sperms during these processes involved arriving at the UVJ, swimming into SSTs and possibly staying inactive in the SST fluid, and eventually capacitating to release from SST. During the later step, the sperms are possibly transferred from inactive to active phase to travel out of the SST tubular epithelium. The mechanisms underlying the intake, maintenance, and release of spermatozoa in SST of UVJ are poorly understood. Many questions are yet to be answered: 1) Why the duration or length of sperm storage is different among the individuals? 2) What are the immediate and long-term molecular responses to the spermatozoa? And 3) What signals trigger or regulate the progressive release of spermatozoa from the SST of UVJ? Most of the previous studies focused on interpreting the gene network regulating the immediate response of UVJ to the sperm intake by comparing mated hens (24 h after mating) with unmated controls using RNA sequencing strategy (Atikuzzaman, et al., 2015; Han, et al., 2019a). It is not surprising that most of the enriched differentially expressed transcripts (lncRNAs, mRNAs, and microRNAs) were highly related with immune- and pH-regulatory genes in UVJ of chicken hens. This mechanism was proved to be conserved among different species because the comparison of UVJ between chicken hens and the counterparts in sows exhibited similar gene regulatory network (Atikuzzaman, et al., 2017). While these studies observed the early impact of

Table 1. The enriched sperm-related genes differentially expressed in the UVJ tissues of white Leghorn hens after insemination (day 9 vs. day 3 after AI).

Genes	Potential function	Expression pattern	Log$_2$ FC[1]	Reference
AGO2	Spermatogenesis-related gene	Seminiferous tubules in rat testis	−0.7723	PMID:27029769
ASB9	Spermatogenesis-related gene	Mouse pachytene spermatocytes and spermatids	−0.6590	PMID: 18776735
CECR2	Spermatogenesis-related gene	Mice testis	−0.7247	PMID:22154806
FGF13	Spermatogenesis-related gene	Mouse testis	−2.6986	PMID: 23554914
LIPG	Spermatogenesis-related gene	Human testis	−0.8166	PMID: 19780863
GFRA1	Related to spermatogenesis (subpopulations of spermatogonia)	Human testis	1.2107	PMID: 28827392
HCK	Spermatogenesis-related gene	Bovine spermatozoa and testis	0.6470	PMID: 17926339
NRG1	Spermatogenesis-related gene	Nrg1(Ser−/−) mutant mice	1.2480	PMID: 18586089
PIP5K1B	Spermatogenesis-related gene	Pip5k1a-knockout, Pip5k1b-Knockout, and Pip5k1a/Pip5k1b double knockout mice	0.5860	PMID: 22321832
SMYD3	Spermatogenesis-related gene	Human testis and spermatozoa	−1.5791	PMID: 16081583
MBOAT1	Related to germline development	Drosophila germ cell	−0.5843	PMID: 19864461
CFTR	Regulate sperm capacitation	Human sperm	0.68207	PMID: 27714810 PMID:19923167
CLIC5	Regulate sperm function	Bovine epididymal spermatozoa	−1.1024	PMID: 15147883
DNAJB1	Chaperone proteins regulating capacitation		0.84846	PMID: 17595329
ERBB4	Related to sperm motility	Erbb4-knockout mice	−1.2368	PMID:29453196 PMID:25058600
LGALS3	Regulate sperm function	Rat, bull testis and epididymis, and human semen prostasomes	0.5908	PMID: 19830550 PMID: 30241677 PMID:19830550
PDE1A	Regulate sperm function	Human and mouse sperm	−0.7014	PMID: 12135876 PMID: 15901640
HES5	Regulates sperm motility by epididymosomes	Mouse epididymis	−1.1295	PMID: 26825631
MLPH	sperm DNA methylation patterns	Human spermatozoal DNA	−0.6076	PMID: 28566207
HIP1	Related to sperm counts and motility	HIP1 knockout mice	0.8861	PMID: 16967501
SFRP1	Regulates spermatid adhesion in the testis	Rats testis	−0.5969	PMID: 23073828
SLC22A18	Responsible for the sperm phenotype	Human sperm	−0.5211	PMID: 25762640
SLC26A8	Sperm tail differentiation and motility	Human and mouse male germ cells	0.5117	PMID: 17517695 PMID: 23582645
FKBP6	Related to male fertility	Equine testis and sperm	1.49906	PMID: 25495881 or 12764197
GDF9	Related to sperm quality	Holstein bulls and bovine Sertoli cells	−1.0501	PMID: 23884762 PMID: 28332739
HDAC4	Related to male infertility (methylation and gene expression)	Human spermatozoal DNA	−0.5727	PMID: 30358834
KRT19	Related to sperm maturation and male fertility	Rat efferent ducts	0.6199	PMID: 19906187
RPL28	Related to fertile and infertile	Human sperm	0.5329	PMID: 25973848
CX3CL1	Related to immune system	Human fallopian tube and ejaculated sperm	−0.7536	PMID: 14747189
EBP	Immune-related genes	Porcine endometrium	0.5559	PMID: 29155178
GPX3	Sperm antioxidant defences	Epididymal fluid in the goat	0.6428	PMID: 27677348
NDRG1	Sperm RNA elements	Human sperm	−0.5120	PMID: 29199464
PDGFRB	Associations with semen production traits	Chinese Holstein bulls	−0.7863	PMID: 28673243
SFMBT1	Associate semen volume and total sperm number	Holstein-Friesian bulls	−0.6057	PMID: 25465359

Abbreviations: AI, artificial insemination; UVJ, uterovaginal junction.
[1]Log2 FC = Log2 foldchange of the gene expression changes day 9 vs. day 3 after AI.

spermatozoa on the sperm reservoir, the followed-up dynamic balance between the maintenance and progressive release of sperms from the UVJ remains largely unclear. Hence, it would be interesting to reveal the mystery of long-term sperm storage in chicken UVJ and to further understand the diversity of sperm reservoir among chicken and other animals. The present study focused on deciphering the molecular network governing the short (3 D) and long length (9 D) of sperm storage in chicken UVJ (day 9 vs. day 3) after mating. The histological analysis of the UVJ revealed sperm bundles in the SST of UVJ collected at day 9 and day 3 time points, whereas the number of bundles greatly reduced at day 9 samples. The morphological changes support the notion

that the spermatozoa experienced progressive release from UVJ over time (Ito, et al., 2011). The observation of spermatozoa in the SST of mated white Leghorn hens (day 9) in our study directly supports the good performance of egg fertility of this egg layer.

During the processes of sperm storage in SST, the potential sperm activation or capacitation requires the complex network including ion (calcium) and pH fluctuation (Holm, et al., 1996; Froman and Feltmann, 2005). The RNA-sequencing was performed to find out what gene network governed this phenomenon. By comparing UVJ tissues (day 9 vs. day 3 after AI) derived from white Leghorn chickens, the enriched 4 GO terms (heparin binding, GAG binding,

Table 2. The differentially expressed genes enriched in gene ontology are potentially related to sperm storage duration.

Description	Count	Differentially expressed genes[1]
Regulation of calcium ion transport	8	ATP2C2, **CEMIP**, LGALS3, **NOS1**, **RAMP3**, **STAC**, STC2, **UBASH3B**
Positive regulation of calcium ion import	4	ATP2C2, **CEMIP**, LGALS3, **RAMP3**
Calcium ion binding	18	**ASPN**, **ASTN2**, **COMP**, ENSGALG00000002553, **ENSGALG00000008326**, **ENSGALG00000012869**, ENSGALG00000014854, **FAT4**, **MAN1C1**, **MCC**, **MMP13**, **PCDH19**, **PLCH2**, **PROS1**, **STYL5**, TESC, THBS4
Regulation of calcium ion import	5	ATP2C2, **CEMIP**, LGALS3, **RAMP3**, **UBASH3B**
Calcium ion import	7	ATP2C2, **CACNA1G**, **CEMIP**, LGALS3, **RAMP3**, **SLC8A1**, **UBASH3B**
Positive regulation of calcium ion transport	4	ATP2C2, **CEMIP**, LGALS3, **RAMP3**
Calcium ion transport	10	ATP2C2, **CACNA1G**, **CEMIP**, LGALS3, **NOS1**, **RAMP3**, **SLC8A1**, **STAC**, STC2, **UBASH3B**
Regulation of metal ion transport	11	ATP2C2, **CEMIP**, LGALS3, **NOS1**, **OSR1**, **RAMP3**, **STAC**, STC2, SNTA1, TESC, **UBASH3B**
Iron ion binding	7	ENSGALG00000020876, HBAA, MELTF, **NOS1**, **SCD**, **TBXAS1**, **XDH**
Regulation of ion transport	15	ATP2C2, **CACNA1G**, **CEMIP**, CFTR, **CLIC5**, LGALS3, **NOS1**, **OSR1**, **PLA2R1**, **RAMP3**, SNTA1, **STAC**, STC2, TESC, **UBASH3B**
Regulation of sodium ion transport	4	**NOS1**, **OSR1**, SNTA1, TESC
Sodium ion transport	7	**FGF13**, **NOS1**, **OSR1**, **SLC8A1**, SLC9A2, SNTA1, TESC
Positive regulation of ion transport	7	ATP2C2, **CEMIP**, CFTR, LGALS3, **PLA2R1**, **RAMP3**, TESC
Sodium ion import	2	**SLC8A1**, SLC9A2
Metal ion transport	18	ATP2C2, **CACNA1G**, **CEMIP**, **FGF13**, LGALS3, MELTF, **NOS1**, **OSR1**, **RAMP3**, **SLC25A37**, SLC39A11, **SLC8A1**, SLC9A2, SNTA1, **STAC**, STC2, TESC, **UBASH3B**
Regulation of sodium ion transmembrane transport	3	**OSR1**, SNTA1, TESC,
Divalent metal ion transport	11	ATP2C2, **CACNA1G**, **CEMIP**, LGALS3, **NOS1**, **RAMP3**, **SLC8A1**, SLC39A11, **STAC**, STC2, **UBASH3B**
Divalent inorganic cation transport	11	ATP2C2, **CACNA1G**, **CEMIP**, LGALS3, **NOS1**, **RAMP3**, **SLC8A1**, SLC39A11, **STAC**, STC2, **UBASH3B**
Sodium ion transmembrane transport	5	**OSR1**, **SLC8A1**, SLC9A2, SNTA1, TESC
Heparin binding	9	**COMP**, **CTGF**, **IMPG2**, PCOLCE, **POSTN**, **RSPO3**, **SFRP1**, **TGFBR3**, THBS4
Response to estradiol	4	**AREG**, **RAMP3**, **SFRP1**, SSTR1,
Glycosaminoglycan binding	10	**CEMIP**, **COMP**, **CTGF**, **IMPG2**, PCOLCE, **POSTN**, **RSPO3**, **SFRP1**, **TGFBR3**, THBS4

[1]The bolded font in the table represents the downregulated differentially expressed genes.

response to estradiol, and regulation of metal ion transport) were predicted to be highly involved with the sperm storage and release.

The concentration of 6 different ions (sodion, phosphonium, sulfion, chloridion, and potassium) was shown to be different between SST tubular fluid and SST epithelial cells of chicken, quail, and turkey hens (Holm, et al., 2000). The sperm motility was regulated by the mitochondrial calcium cycling driven by extracellular sodium (Froman and Feltmann, 2005). The fluctuation of ions in the SST fluid may be one of the drivers for sperm maintenance in or release from SST. Our analyses confirmed this observation from molecular level by enriching a series of solute carrier family genes represented by solute carrier family genes (*SLC8A1*, *SLC16A5*, *SLC22A18*, *SLC26A8*, and *SLC43A2*) that may function in transporting lactic acid, hydrogen, and calcium ions (Hediger, et al., 2004; Perland and Fredriksson, 2017). *SLC43A2* is an amino acid transporter mainly mediating the exchange of amino acids across the placental membrane to the fetus. Solute carrier family 26 member 8 (*SLC26A8*) is one of 11 members of the *SLC26* family (solute carrier family) that interacts with *CFTR* to transport anions required for sperm motility and capacitation (Fong, 2012; Dirami, et al., 2013). *CFTR* is involved in regulating Cl^- and HCO_3^- transport and secretion in epithelial lining tissues including reproductive tracts. Activation of *CFTR* is responsible for the sustained uptake of HCO_3^- into sperms to trigger the sperm capacitation

when exposed to high concentration of HCO_3^- in seminal plasma or reproductive tract (Riordan, et al., 1989; Wang, et al., 2003; Muchekehu and Quinton, 2010). The lower expression of *CFTR* in chicken UVJ tissues at day 3 after AI was supposed to reduce the sperm capacitation in SST, whereas the acidic fluid in SST also contributed to the sperm inactivation.

The response to estradiol GO terms (*RAMP3*) and calcium signaling pathway (*CACNA1G*, *ERBB4*, *HTR7*, *NOS1*, *PDE1C*, *PDGFRB*, and *SLC8A1*) were enriched in our data. Estradiol, particularly E2 (17β-estradiol), was shown to have a negative impact on the binding of bovine oviduct epithelial cells to spermatozoa in cell culture systems (Lamy, et al., 2017; Yoshimoto, et al., 2017). The administration of estradiol triggered adrenomedullin to induce uterine artery relaxation by increasing *RAMP3* expression (Ross, et al., 2010). *RAMP3* acts as chaperone to assist the activation of adrenomedullin which increases the concentration of intercellular calcium ions and maintains the ion microenvironment in rat oviduct. *RAMP3* was shown to express both in the ciliated and secretory cells of the ampullary tissue of bovine oviduct and regulate the oviductal fluid flow, particularly to release calcium from intracellular storage (Yoshimoto, et al., 2017). *SLC8A1*, a calcium extrusion regulatory molecule encoding the NCX1 antiporter member protein, was shown to regulate the calcium homeostasis. The dysregulation of NCX1 was highly associated with heart failure and Kawasaki disease caused by impaired calcium flux (Shimizu, et al.,

Table 3. The differentially expressed genes enriched in different signaling pathways are potentially related with sperm storage duration.

Pathway	Count	Differentially expressed genes[1]
Calcium signaling pathway	7	**CACNA1G, ERBB4, HTR7, NOS1, PDE1C, PDGFRB, SLC8A1**
Glycosaminoglycan biosynthesis	4	**B3GNT7, CSGALNACT1, GLCE, ST3GAL1**
ECM-receptor interaction	6	**SDC1, FN1, ITGB6, VTN, COMP,** THBS4

Abbreviation: ECM, extracellular matrix.
[1]The bolded font in the table represents the downregulated differentially expressed gene.

2016). The downregulation of *SLC8A1* implied that the sperm release from the reservoir was highly correlated with calcium extrusion. *STAC* was identified as a new regulatory family functioned in voltage-gated calcium channel trafficking (Campiglio, et al., 2018). The downregulation of *RAMP3*, *SLC8A1*, and *STAC* indicated the potential roles involved in high calcium concentration in SST to maintain the sperm to be inactive. *PDE1C* is calcium/calmodulin-dependent phosphodiesterase that was highly related to male mating behavior and infertility in *Drosophila melanogaster* (Morton, et al., 2010). Although *PDE1C* male mutants with decreased expression displayed normal spermatogenesis and maturation, they were presumably not favored by the females in courtship behavior. The normal females that successfully mated with *PDE1C* male mutants showed normal sperm maintenance in uterus 24 h after mating and few sperms in seminal receptacle (sperm reservoir) 72 h after mating comparing with those of control group with abundant sperm distribution. The greatly decreased sperm storage in seminal receptacle implied that *PDE1C* was functionally important for female sperm storage in sperm reservoir with unknown mechanisms. The downregulation of *PDE1C* gene with nearly 1.5 folds (UVJ day 9 vs. day 3 after AI) in our sequencing data highly implied that *PDE1C* expression pattern was positively correlated with the duration of spermatozoa in UVJ of hens. *HIP1* is an endocytic membrane adaptor protein that is involved in clathrin-mediated endocytosis. The *HIP1* mutant mice displayed obvious defects in testis with 50% reduction of sperm production comparing with those of controls. The most interesting observation was the increase of static sperm by 143% and decrease of sperm velocity by 25% in *HIP1* mutant mice (Rao, et al., 2001; Khatchadourian, et al., 2007). These data highly indicate that *HIP1* was
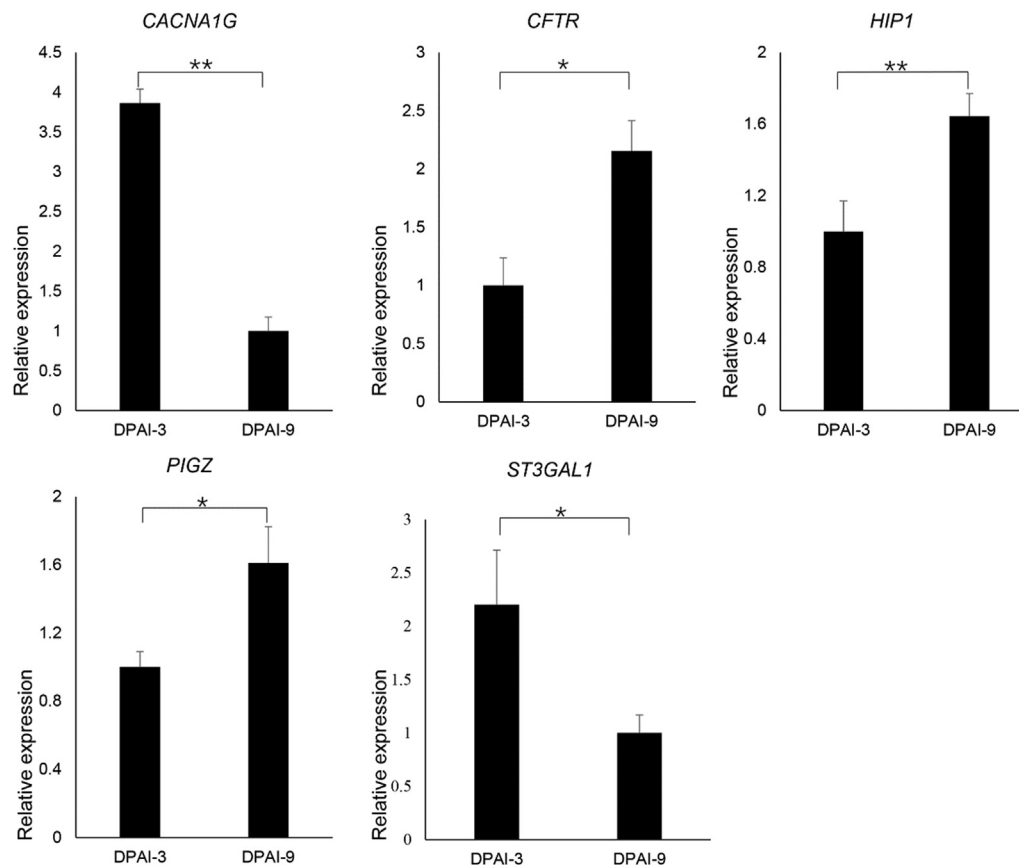

Figure 3. The quantitative real-time PCR validation of randomly selected differentially expressed genes (*CACNA1G, CFTR, HIP1, ST3GAL1,* and *PIGZ*) in mated chicken uterovaginal junction folds (day 9 vs. day 3 after artificial insemination [AI]). Day post-AI (DPAI)-3 represented day 3 post-AI group (n = 5), whereas DPAI-9 represented day 9 post-AI group (n = 6). Error bars represented SEM. "*" and "**" represented the levels of significant differences at $P < 0.05$ and $P < 0.01$, respectively.

positively correlated with the sperm activity. The upregulation of *HIP1* gene expression in UVJ tissue (day 9 vs. day 3 after AI) suggested that the low expression of *HIP1* helps the spermatozoa to keep quiescence for short-term maintenance in SST of UVJ in day 3 samples.

The GAG unit has been identified in different parts of the chicken oviduct including SST to potentially function in regulating sperm storage process (Trainis, 1967; Bakst and Bauchan, 2016). GAG were reported to have crucial roles in stimulating acrosome reactions in bovine, porcine, and rabbit sperms in vitro. The GAG heparin worked as the most potent inducer of capacitation in bovine and ovine female reproductive tracts (Handrow, et al., 1982; Handrow, et al., 1984; Therien, et al., 2005). The *ST3GAL1* gene was an important enzyme in GAG biosynthesis. The *ST3GAL1* gene was differentially expressed in UVJ tissues (day 9 vs. day 3 after AI) and enriched in GAG binding and heparin in GO analysis, indicating its potential roles in sperm functional regulation, such as metabolic activity, motility, and acrosomal enzyme activity.

In conclusion, the sperms stored in SST of chicken UVJ were decreasing overtime (day 9 vs. day 3) after insemination. The enrichment of ion-related genes and cell migratory–related genes implied their important roles in maintaining and releasing the sperms in and from the SST of UVJ. A series of genes such as *RAMP3*, *PDE1C*, *HIP1*, and *ST3GAL1* may be candidates to further study the short and long length of sperm storage in sperm reservoir of chicken hens. This is the first report addressing the global gene expression correlated with relatively long-term sperm storage in chicken hens. The molecular network identified in this report will contribute to further explore the differential capacity of sperm storage among individuals and eventually understand the diversity of the sperm storage displayed in different breeds and species of female animals in nature.

ACKNOWLEDGEMENTS

SUPPLEMENTARY DATA

Supplementary data associated with this article can be found in the online version at https://doi.org/10.1016/j.psj.2019.10.021.

REFERENCES

Atikuzzaman, M., M. Alvarez-Rodriguez, A. Vicente-Carrillo, M. Johnsson, D. Wright, and H. Rodriguez-Martinez. 2017. Conserved gene expression in sperm reservoirs between birds and mammals in response to mating. BMC Genomics 18:98.

Atikuzzaman, M., R. Mehta Bhai, J. Fogelholm, D. Wright, and H. Rodriguez-Martinez. 2015. Mating induces the expression of immune- and pH-regulatory genes in the utero-vaginal junction containing mucosal sperm-storage tubuli of hens. Reproduction 150:473–483.

Bakst, M. R., and V. Akuffo. 2007. Alkaline phosphatase reactivity in the vagina and uterovaginal junction sperm-storage tubules of turkeys in egg production: implications for sperm storage. Br. Poult. Sci. 48:515–518.

Bakst, M. R., and G. Bauchan. 2015. Apical blebs on sperm storage tubule epithelial cell microvilli: their release and interaction with resident sperm in the Turkey hen oviduct. Theriogenology 83:1438–1444.

Bakst, M. R., and G. Bauchan. 2016. Lectin staining of the uterovaginal junction and sperm-storage tubule epithelia in broiler hens. Poult. Sci. 95:948–955.

Bakst, M. R., G. J. Wishart, and J. P. Brillard. 1994. Oviducal sperm selection, transport, and storage in poultry. Poult.sci.rev 5:117–143.

Bobr, L. W., F. W. Lorenz, and F. X. Ogasawara. 1964. Distribution of spermatozoa in the oviduct and fertility in domestic birds. I. Residence sites of spermatozoa in Fowl oviducts. J. Reprod. Fertil. 8:39–47.

Campiglio, M., P. Coste de Bagneaux, N. J. Ortner, P. Tuluc, F. Van Petegem, and B. E. Flucher. 2018. STAC proteins associate to the IQ domain of CaV1.2 and inhibit calcium-dependent inactivation. Proc. Natl. Acad. Sci. U S A. 115:1376–1381.

Das, S. C., N. Isobe, and Y. Yoshimura. 2010. Analysis of changes in the expression of transforming growth factor-βs in the uterovaginal junction of hen oviduct in response to sperm Concerning their significance in sperm Survivability. J. Poult. Sci. 47:326–332.

Dirami, T., B. Rode, M. Jollivet, N. Da Silva, D. Escalier, N. Gaitch, C. Norez, P. Tuffery, J. P. Wolf, F. Becq, P. F. Ray, E. Dulioust, G. Gacon, T. Bienvenu, and A. Toure. 2013. Missense mutations in SLC26A8, encoding a sperm-specific activator of CFTR, are associated with human asthenozoospermia. Am. J. Hum. Genet. 92:760–766.

Fong, P. 2012. CFTR-SLC26 transporter interactions in epithelia. Biophys. Rev. 4:107–116.

Foye-Jackson, O. T., J. A. Long, M. R. Bakst, L. A. Blomberg, V. G. Akuffo, M. V. B. Silva, H. D. Guthrie, and J. P. Mcmurtry. 2011. Oviductal expression of avidin, avidin-related protein-2, and progesterone receptor in Turkey hens in relation to sperm storage: effects of oviduct tissue type, sperm presence, and Turkey line. Poult. Sci. 90:1539–1547.

Froman, D. P., and A. J. Feltmann. 2005. Fowl (Gallus domesticus) sperm motility depends upon mitochondrial calcium cycling driven by extracellular sodium. Biol. Reprod. 72:97–101.

Gilbert, A. B., M. E. Reynolds, and F. W. Lorenz. 1968. Distribution of spermatozoa in the oviduct and fertility in domestic birds. V. Histochemistry of the uterovaginal sperm-host glands of the domestic hen. J. Reprod. Fertil. 16:433–444.

Han, J., H. I. Ahmad, X. Jiang, and G. Liu. 2019a. Role of genome-wide mRNA-seq profiling in understanding the long-term sperm maintenance in the storage tubules of laying hens. Trop. Anim. Health Prod.

Han, J., H. I. Ahmad, X. Jiang, and G. Liu. 2019b. Role of genome-wide mRNA-seq profiling in understanding the long-term sperm maintenance in the storage tubules of laying hens. Trop. Anim. Health Prod. 51:1441–1447.

Handrow, R. R., S. K. Boehm, R. W. Lenz, J. A. Robinson, and R. L. Ax. 1984. Specific binding of the glycosaminoglycan 3H-heparin to bull, monkey, and rabbit spermatozoa in vitro. J. Androl. 5:51–63.

Handrow, R. R., R. W. Lenz, and R. L. Ax. 1982. Structural comparisons among glycosaminoglycans to promote an acrosome reaction in bovine spermatozoa. Biochem. Biophys. Res. Commun. 107:1326–1332.

Hediger, M. A., M. F. Romero, J. B. Peng, A. Rolfs, H. Takanaga, and E. A. Bruford. 2004. The ABCs of solute carriers: physiological, pathological and therapeutic implications of human membrane transport proteinsIntroduction. Pflugers Arch. 447:465–468.

Holm, L., H. Ekwall, G. J. Wishart, and Y. Ridderstrale. 2000. Localization of calcium and zinc in the sperm storage tubules of chicken, quail and Turkey using X-ray microanalysis. J. Reprod. Fertil. 118:331–336.

Holm, L., Y. Ridderstrale, and P. G. Knutsson. 1996. Localisation of carbonic anhydrase in the sperm storing regions of the domestic hen oviduct. Acta Anat. (basel) 156:253–260.

Holt, W. V., and A. Fazeli. 2016. Sperm storage in the female reproductive tract. Annu. Rev. Anim. Biosci. 4:291–310.

Huang, A., N. Isobe, T. Obitsu, and Y. Yoshimura. 2016. Expression of lipases and lipid receptors in sperm storage tubules and possible role of fatty acids in sperm survival in the hen oviduct. Theriogenology 85:1334–1342.

Ito, T., N. Yoshizaki, T. Tokumoto, H. Ono, T. Yoshimura, A. Tsukada, N. Kansaku, and T. Sasanami. 2011. Progesterone is a sperm-releasing factor from the sperm-storage tubules in birds. Endocrinology 152:3952–3962.

Khatchadourian, K., C. E. Smith, M. Metzler, M. Gregory, M. R. Hayden, D. G. Cyr, and L. Hermo. 2007. Structural abnormalities in spermatids together with reduced sperm counts and motility underlie the reproductive defect in HIP1-/- mice. Mol. Reprod. Dev. 74:341–359.

Lamy, J., E. Corbin, M. C. Blache, A. S. Garanina, R. Uzbekov, P. Mermillod, and M. Saint-Dizier. 2017. Steroid hormones regulate sperm-oviduct interactions in the bovine. Reproduction 154:497–508.

Matsuzaki, M., S. Mizushima, G. Hiyama, N. Hirohashi, K. Shiba, K. Inaba, T. Suzuki, H. Dohra, T. Ohnishi, Y. Sato, T. Kohsaka, Y. Ichikawa, Y. Atsumi, T. Yoshimura, and T. Sasanami. 2015. Lactic acid is a sperm motility inactivation factor in the sperm storage tubules. Sci. Rep. 5:17643.

Matsuzaki, M., and T. Sasanami. 2017. Sperm storage in the female reproductive tract: a conserved reproductive strategy for Better fertilization success. Adv. Exp. Med. Biol. 1001:173–186.

Morton, D. B., R. Clemens-Grisham, D. J. Hazelett, and A. Vermehren-Schmaedick. 2010. Infertility and male mating behavior deficits associated with Pde1c in Drosophila melanogaster. Genetics 186:159–165.

Muchekehu, R. W., and P. M. Quinton. 2010. A new role for bicarbonate secretion in cervico-uterine mucus release. J. Physiol. 588:2329–2342.

Perland, E., and R. Fredriksson. 2017. Classification systems of Secondary active transporters. Trends Pharmacol. Sci. 38:305–315.

Rao, D. S., J. C. Chang, P. D. Kumar, I. Mizukami, G. M. Smithson, S. V. Bradley, A. F. Parlow, and T. S. Ross. 2001. Huntingtin interacting protein 1 Is a clathrin coat binding protein required for differentiation of late spermatogenic progenitors. Mol. Cell Biol 21:7796–7806.

Riordan, J. R., J. M. Rommens, B. Kerem, N. Alon, R. Rozmahel, Z. Grzelczak, J. Zielenski, S. Lok, N. Plavsic, and J. L. Chou, et al. 1989. Identification of the cystic fibrosis gene: cloning and characterization of complementary DNA. Science 245:1066–1073.

Ross, G. R., U. Yallampalli, P. R. Gangula, L. Reed, K. Sathishkumar, H. Gao, M. Chauhan, and C. Yallampalli. 2010. Adrenomedullin relaxes rat uterine artery: mechanisms and influence of pregnancy and estradiol. Endocrinology 151:4485–4493.

Shimizu, C., H. Eleftherohorinou, V. J. Wright, J. Kim, M. P. Alphonse, J. C. Perry, R. Cimaz, D. Burgner, N. Dahdah, L. T. Hoang, C. C. Khor, A. Salgado, A. H. Tremoulet, S. Davila, T. W. Kuijpers, M. L. Hibberd, T. A. Johnson, A. Takahashi, T. Tsunoda, M. Kubo, T. Tanaka, Y. Onouchi, R. S. Yeung, L. J. Coin, M. Levin, and J. C. Burns, International Kawasaki Disease Genetics. 2016. Genetic Variation in the SLC8A1 calcium signaling pathway is associated with Susceptibility to Kawasaki disease and Coronary artery abnormalities. Circ. Cardiovasc. Genet. 9:559–568.

Sullivan, R., and F. Saez. 2013. Epididymosomes, prostasomes, and liposomes: their roles in mammalian male reproductive physiology. Reproduction 146:R21–R35.

Therien, I., A. Bergeron, D. Bousquet, and P. Manjunath. 2005. Isolation and characterization of glycosaminoglycans from bovine follicular fluid and their effect on sperm capacitation. Mol. Reprod. Dev. 71:97–106.

Trainis, K. V. 1967. [Mucopolysaccharides of the oviduct wall in the laying hen]. Arkh Anat. Gistol Embriol 53:102–107.

Wang, X. F., C. X. Zhou, Q. X. Shi, Y. Y. Yuan, M. K. Yu, L. C. Ajonuma, L. S. Ho, P. S. Lo, L. L. Tsang, Y. Liu, S. Y. Lam, L. N. Chan, W. C. Zhao, Y. W. Chung, and H. C. Chan. 2003. Involvement of CFTR in uterine bicarbonate secretion and the fertilizing capacity of sperm. Nat. Cell Biol 5:902–906.

Yoshimoto, Y., T. Nishie, S. Ito, Y. Kobayashi, Y. Yamamoto, K. Okuda, and K. Kimura. 2017. Adrenomedullin regulates the speed of oviductal fluid flow in cattle. Mol. Reprod. Dev. 84:712–718.

Zaniboni, L., and M. R. Bakst. 2004. Localization of aquaporins in the sperm storage tubules in the Turkey oviduct. Poult. Sci. 83:1209–1212.